Center for the Study of Institutional Diversity

CSID Working Paper Series

#CSID-2012-009

The Topology of Non-Linear Global Carbon Dynamics: From Tipping Points to Planetary Boundaries

John M. Anderies
Arizona State University, USA

S.R. Carpenter
Center for Limnology, University of Wisconsin, Madison WI 53706, USA

Will Steffen
Australian National University, Canberra, ACT, Australia

Johan Rockstrom
Stockholm Resilience Center, Stockholm, Sweden

August 20, 2012

The Center for the Study of Institutional Diversity resides in the School of Human Evolution and Social Change at Arizona State University. CSID can be found on the internet at: http://csid.asu.edu. CSID can be reached via email at csid@asu.edu.

The Topology of Non-Linear Global Carbon Dynamics: From Tipping Points to Planetary Boundaries

John M. Anderies[a], S.R. Carpenter[b], Will Steffen[c], Johan Rockstrom[d]

[a]Center for the Study of Institutional Diversity, Arizona State University, Tempe, AZ 85287-2402, USA;
[b]Center for Limnology, University of Wisconsin, Madison WI 53706, USA;
[c]Australian National University, Canberra, ACT, Australia ;
[d]Stockholm Resilience Center, Stockholm, Sweden;

Corresponding author:
John M. Anderies
School of Human Evolution and Social Change
School of Sustainability
Arizona State University
PO Box 87402
Tempe, AZ 85287-2402, USA
m.anderies@asu.edu

Abstract:
This paper develops a minimal model of land use and carbon cycle dynamics and explores the relationship between nonlinear dynamics and planetary boundaries. Only the most basic interactions between land cover, terrestrial carbon stocks and atmospheric carbon stocks are considered. The goal is not to predict global carbon dynamics as it occurs in the actual earth system, but rather, to construct a conceptually reasonable representation of a feedback system between different carbon stores like that of the actual earth system and use it to explore the topology of the boundaries of what can be called a safe operating space" for humans. The analysis of the model illustrates the potential complexity of planetary boundaries and highlights some challenges associated with navigating them.

Keywords:

The Topology of Non-Linear Global Carbon Dynamics: From Tipping Points to Planetary Boundaries

J. M. Anderies[1], S. R. Carpenter[2], Will Steffen[3,4], and Johan Rockström[4]

This paper develops a minimal model of land use and carbon cycle dynamics and explores the relationship between nonlinear dynamics and planetary boundaries. Only the most basic interactions between land cover, terrestrial carbon stocks and atmospheric carbon stocks are considered. The goal is not to predict global carbon dynamics as it occurs in the actual earth system, but rather, to construct a conceptually reasonable representation of a feedback system between different carbon stores like that of the actual earth system and use it to explore the topology of the boundaries of what can be called a "safe operating space" for humans. The analysis of the model illustrates the potential complexity of planetary boundaries and highlights some challenges associated with navigating them.

1. Introduction

Increasing human pressure on ecosystem processes coupled with global change has raised recent concerns about human societies approaching boundaries or "tipping points" that, once crossed, may induce fundamental shifts in Earth System dynamics [*Lenton et al.*, 2008; *Kerr*, 2008]. *Rockström et al.* [2009] have identified 9 such boundaries and provided a rough estimate of the position of the present planetary system. The authors suggest that three boundaries (biodiversity loss, biogeochemical flows of nitrogen, and atmospheric carbon dioxide concentration) may have already been crossed and that we are nearing several others.

These estimates do not yet consider the interaction between boundaries; approaching one boundary may cause others to shift. Understanding how these boundaries interact and respond to changes in the system state is an important area of research. There have been attempts to estimate boundaries for global systems [*Rahmstorf*, 1995] and the computational and data demands are substantial. In such situations, simple heuristic models can help organize questions and explore interactions that can eventually be addressed using large data sets or more realistic models [*Lenton*, 2000; *Petoukhov et al.*, 2000; *Randall et al.*, 2007].

We employ this strategy to explore the relationship between atmospheric CO_2 and landuse change boundaries. We consider only the most basic interactions between terrestrial, marine and atmospheric carbon stocks. The goal is not to predict but, rather, to construct a conceptually reasonable model of a feedback system *like* that of the actual Earth System and use it to explore the topology of the boundaries of a safe operating space (SOS) for humans. We characterize the topology of basins of attraction for stable climate configurations and assess their sensitivity to landuse change, ocean acidification, and the release of fossil carbon into the atmosphere.

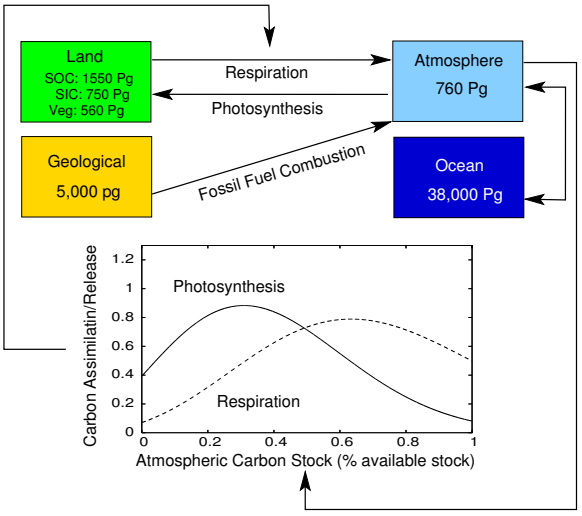

Figure 1. Minimal model depiction of the Earth System in terms of the feedback between atmospheric carbon stocks and carbon flux rates between terrestrial and atmospheric stocks. (stock data from *Lal* [2003].)

2. The model

Our Earth System model is similar in spirit to that of *Lenton* [2000] and captures interactions between Net Ecosystem Production (NEP) and carbon stocks (Figure 1). Given our focus on the *topology* of carbon dynamics, we employ mathematical functions that capture the essential shape of empirical relationships. As such, our modeling exercise departs somewhat from more empirically based efforts [e.g. *Lenton*, 2000] but the qualitative model dynamics are similar. This allows us to focus on implications of basic relationships that are robust to a wide range of parameter choices. Space limitations allow only a brief overview of the model here. Please see the supplementary material for a detailed discussion of the model.

The model is a simple mass balance that tracks the carbon stocks and the fluxes using the following system of ordinary

[1]School of Sustainability and School of Human Evolution and Social Change. Arizona State University. Email: m.anderies@asu.edu

[2]Center for Limnology, University of Wisconsin, Madison Wisconsin

[3]Australian National University, Canberra, ACT, Australia

[4]Stockholm Resilience Center, Stockholm Sweden

differential equations

$$\frac{dc_t}{d_t} = NEP(p(T, c_a(t)), r(T), c_t(t)) - H(t) \quad (1)$$

$$\frac{dc_m}{dt} = D(c_a(t), c_m(t)) \quad (2)$$

$$\frac{dC}{dt} = I(t) \quad (3)$$

where $c_t(t)$, $c_m(t)$, $c_a(t)$, and C represent terrestrial, marine, atmospheric and total *available* carbon stocks at time t, respectively. Note, we assume that $c_t(t)+c_m(t)+c_a(t) = C(t)$ so that $c_a(t)$ is determined by the other three stocks. The change in $c_t(t)$ depends on net ecosystem production, NEP, and human activities such as fires, tilling soil, and landuse change that may release terrestrial carbon, $H(t)$. NEP is a function photosynthesis rate, $p(T, c_a)$, respiration rate, $r(T)$, and of c_t itself (e.g. plant biomass available to photosynthesize and respirate). These rates are, in turn, dependent on global mean average temperature, T (Figure S2A, supplementary material). Given that T depends on c_a, we can relate $p(T, c_a)$ and $r(T)$ directly to c_a as shown in Figure 1. Note that p depends directly on c_a as well due to fertilization effects. Finally, we assume that the flux between atmospheric and marine stocks, $D(c_a, c_m)$, depends on their difference. We let $D(c_a, c_m) = a_m(c_a - c_m)$, the simplest possible representation of this diffusion process. The rate constant, a_m, could depend on c_m (ocean acidification) with important implications (see Section 4).

Global change is captured via human activities that 1) release trapped geological carbon through an industrialization process described by $I(t)$ and 2) affect c_a and c_m through the release of terrestrial carbon stocks. In Section 2, we conduct a full analysis to define a SOS for humanity. However, to provide intuition we present an analysis of the model considering only terrestrial and atmospheric carbon in the supplementary material. This analysis isolates the roles of photosynthesis, respiration, and density dependent factors in terrestrial systems. Specifically, considering only photosynthesis and respiration leads to a system that, depending on initial conditions, will either converge to a state with high c_t, low c_a, a cold climate, and very low rates of photosynthesis and respiration (perpetual tundra) or to a global "desert state" with $c_t = 0$ and an extremely hot climate (see Figure S3B, supplementary material). Adding density dependence (e.g. plants compete for a limited resource such as water) resolves this unrealistic situation by introducing a new stable equilibrium at $c_a = k$ where k is the carrying capacity of terrestrial biomass (see Figure S4A, supplementary material). Here, the notion of a (one-dimensional) SOS becomes clear. If $c_a(t)$ remains above the boundary, the system will tend toward an equilibrium with $c_a > 0$. Otherwise, it will converge to the global desert state ($c_a \to 0$). Figure S4B shows the affect of an annual proportional carbon offtake by humans, i.e. when $H(t) = \alpha c_t(t)$. As α increases, the SOS shrinks and eventually vanishes. We can compute when this occurs (peak of curve falls below horizontal - i.e. red curve, Figure S4B) using bifurcation techniques. If α exceeds 26% of terrestrial carbon stocks, the system enters the "hot desert" (HD) basin.

3. Analysis

To begin, we treat C as a parameter (i.e. $I(t) = 0$) and explore how varying C and human terrestrial biomass offtake rate, α, affects the topology of the Earth System model. This reduces the system to a 2-dimensional model in (c_t, c_m) phase space, allowing for a clearer representation of model topology. In Section 4 we relax this assumption and allow C to vary over time. We rescale C so that its default value of "1" corresponds to roughly 4,500 gigatons of carbon with 750, 2850, and 900 in the atmosphere, terrestrial systems, and surface ocean, respectively [IPCC AR4 WG1, *Lal*, 2003]. These choices of units have no effect on the dynamics and are meant only to orient readers. Likewise, the temperature scale is arbitrary and the one shown in Figure S2A was chosen to correspond to those in the literature. What is key is the mapping from atmospheric carbon stocks to photosynthesis and respiration rates as shown in Figure 1. Given the uncertainty around the carbon-global mean temperature relationship, we assume it is linear with slope a_T, intercept b_T, and explore the effect of varying these parameters on the model. Finally, the parameters r_{tc}, a_m, and α simply set the time scale; it is only their *relative* values, especially with regard to α (which we vary in our analysis) that are important determinants of the dynamics. In the analysis that follows, we set $r_{tc} = 2.5$ and $a_m = 0.05$.

Figure 2 summarizes the dynamics of the model. Panel A is a phase-plane diagram of marine versus terrestrial carbon. The green and red lines are the c_m and c_t-isoclines, respectively. The slanted c_t-isocline is the locus of points where the photosynthesis and respiration curves intersect: to the right of this line, the terrestrial system accumulates carbon and to the left, it loses carbon. The vertical c_t-isocline is located at the terrestrial carbon carrying capacity. The c_m-isocline is the locus of points for which $D(c_a, c_m) = 0$, or equivalently, $c_m = c_a$. Two trajectories are shown for different initial conditions. Panels D and E show time trajectories for phase plane trajectories 1 and 2, respectively. There is one, globally stable equilibrium where the isoclines intersect (black circle in Panel A) where $c_t = 0.6$ (2,400 gT), $c_a = 0.2$ (800 gT), and $c_m = 0.2$ (800 gT) so the system can *always* return to this equilibrium (roughly present conditions) from any perturbation. However, if the perturbation is large (trajectory 2), the system will take a long excursion (panel E) with almost zero terrestrial carbon (sustained hot desert) before recovering in contrast to the quick recovery in panel D. The region in which the system recovers quickly (the SOS) is shaded grey.

Panels B and C in Figure 2 illustrate the impact of human appropriation of terrestrial carbon stocks (α). The geometry of the c_t-isocline is fundamentally different for the case when $\alpha = 0.3$ (Panel B) than when $\alpha = 0.5$ (Panel C). As α increases, the SOS shrinks (compare size of the grey region *and* the horizontal distance from equilibrium to the lower branch of the c_t-isocline in Panels A, B and C). Further, the stability of the equilibrium at $(c_t, c_m, c_a) = (0, 0.5, 0.5)$ (i.e. no terrestrial carbon) changes. For both values of α, the time path of trajectory 1 is similar to that shown in Figure 2D. For $\alpha = 0.3$, the time path of trajectory 2 would be similar to that in Figure 2E: the system takes a long excursion through a region in state space with almost no terrestrial carbon before it recovers. This is due to the fact that when $\alpha = 0.3$, the equilibrium point at $(c_t, c_m, c_a) = (0, 0.5, 0.5)$ is an unstable saddle (Figure 2B). In contrast, when $\alpha = 0.5$ (Figure 2C), this equilibrium is a stable node (a saddle-node bifurcation occurs between $\alpha = 0.3$ and $\alpha = 0.5$). In this case, trajectory 2 will be absorbed into this node and the system will never recover. This is unlikely, as humans could never harvest the very last unit of terrestrial biomass. However, other biological factors (e.g. Allee effect) may generate thresholds beyond which terrestrial systems can no longer capture carbon.

We now consider how SOS boundaries interact. There are two types of boundaries to consider. The grey regions in Figure 2A-C show *state variable* boundaries (basins of attraction) for a given, *fixed* parameter that determine the

size of perturbations (a sudden huge fire or severe drought) the system can tolerate (state remains in grey region). Figure 2A-C shows how the SOS shrinks as α increases, *ceteris paribus*. In reality, how the SOS changes as α increases is affected by other parameters. For example, total carbon, C, affects the maximum value of α for which there exists a stable equilibrium with $c_t > 0$ with its associated basin of attraction. Thus, there are *parameter value* boundaries across which the system behavior fundamentally changes (stable equilibrium and basin of attraction with positive c_t vanish). We can compute the boundary in $C - \alpha$ parameter space for which this occurs (Figure 2F). For parameter combinations In the region labelled "PE" (**p**ositive **e**quilibrium) trajectories will follow paths of type 1 or 2 as in Figure 2A, always returning to a stable equilibrium with $c_t > 0$. Parameter combinations in the "ZE" (**z**ero **e**quilibrium) region will generate trajectories that will *always* converge to a stable equilibrium with zero terrestrial carbon stocks (type 2 paths as in Figure 2C).

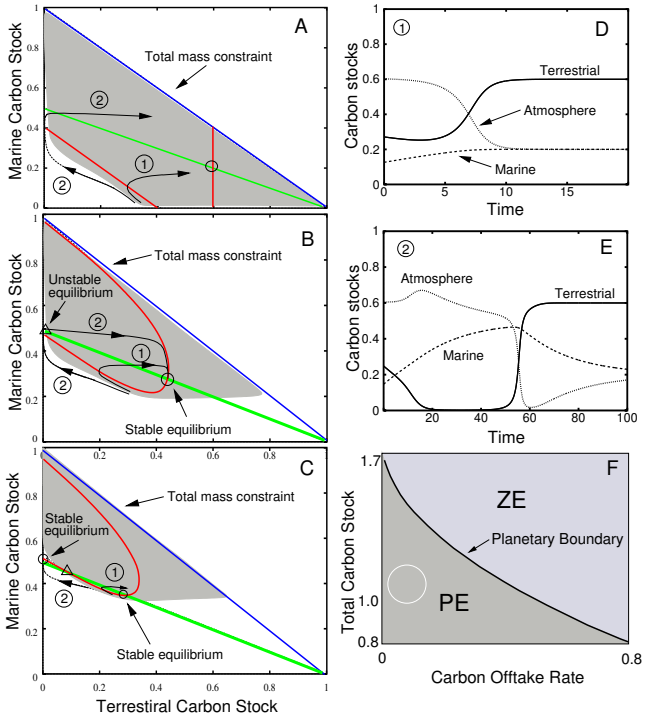

Figure 2. A-C: Phase plane analysis of the full model (Note: total carbon is treated as a parameter, thus the total mass constraint reduces the model from 3 physical to 2 mathematical dimensions) with $\alpha = 0$ (A), $\alpha = 0.3$ (B), and $\alpha = 0.5$ (C). The state space basin boundaries (grey regions) are shown for each case. D-E: Examples of time trajectories associated with the phase space trajectories of type 1 and 2 for the case shown in A, respectively. F: Two parameter map showing combinations of C and α for which a positive stable equilibrium does (PE region) or does not (ZE region) exist. See text for discussion.

If we believe this model and our parameterization, our present state probably lies somewhere in the white circle - quite far from the total carbon–terrestrial carbon appropriation rate boundary. However, the location of the boundary is sensitive to parameter choices. Can we detect when we are approaching a boundary? As can be seen from Figures 2B and C in which type 1 and 2 trajectories start very close to one another and diverge at a later time, this can be devilishly difficult. Given the time scales involved, the system could be on a type 2 trajectory for a very long time before it would become clear, based only on measurements of the system state, that the system was in the ZE region. Figure 2 illustrates how boundaries relevant on longer time scales (parameter value boundaries) interact and influence boundaries relevant on shorter time scales (state variable boundaries).

4. Detecting boundaries in practice

Our analysis suggests that the model topology resembles a ball rolling on the "climate sheet" in the c_t-c_m plane with two basins (one good, one bad). Releasing carbon and clearing land tilts the sheet in the climate game. Our analysis tells us how far we can tilt the climate sheet without falling into the bad basin (Figure 2F), and how parameters affect the shape of the basins. This analogy highlights momentum effects: how fast the sheet is tilted (acceleration of ball) affects how far it can be tilted before the ball leaves the basin, i.e. the climate system is sensitive not only to the the *amount* of carbon released into the atmosphere, but also at what *rate* it is released. This general topological view provides important policy design principles: 1) reducing emission rate may be beneficial regardless of the total eventual level of c_a, and 2) understanding other feedbacks that influence parameters in our model is critical. We illustrate this point with three model scenarios.

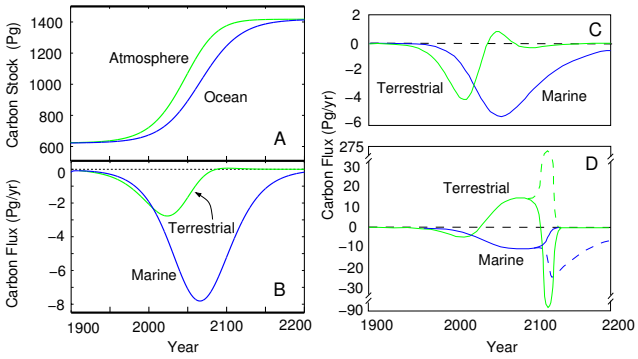

Figure 3. Industrialization scenarios. A: Atmospheric and ocean carbon stocks and B: Net fluxes between the atmosphere and the terrestrial and marine systems. For A and B: All parameters are the same is in the topological analysis except $\alpha = 0.1$, $a_m = 0.04$, $r_{tc} = 1.5$, $c_f = 2$, $b_f = 0.5$, $r_i = 0.04$, $c_{max} = 0.4$, and $k = 0.8$. C-D: Scenarios with ocean acidification, additional terrestrial carbon, and 50% faster carbon release from fossil fuels. Parameters - same as B except $\alpha = 0.15$, $a_m = 0.01$, $r_i = 0.06$.

Figure 3A-B shows a scenario in which $C(t)$ mimics Earth's industrialization since 1900. Assuming industrialization is the only source of additional carbon, we have $C(t) = C_o + C_r(t)$ where C_o is the total carbon stock when industrialization begins and $C_r(t)$ is the carbon released by industrialization. The dynamics of $C_r(t)$ are modeled as a logistic - i.e. $I(t) = dC_r(t)/dt = r_i C_r(1 - C_r/c_{max})$ where r_i sets the pace for industrialization and c_{max} sets the total carbon released when a global agreement on emissions

is reached (see caption for parameter values). The scenario begins at a pre-industrial equilibrium with $c_m = c_a = 620$ Pg, and $c_t = 2895$ (0.138 and 0.643 in non-dimensional variables). We assume that society successfully reduces fossil carbon emissions to zero by 2100 (Figure 3A) when $c_a(t)$ stabilizes at roughly twice the pre-industrial level. The way in which the marine and terrestrial systems process this signal, in terms of net carbon fluxes is shown in Figure 3B. These flux scenarios are a good qualitative match with those generated by a range of other more detailed models [*Cramer et al.*, 2001; *Prentice et al.*, 2001]. Early in the scenario, increasing atmospheric carbon increases photosynthesis both through the temperature and fertilization effect and, in turn, increases terrestrial carbon uptake (terrestrial system is a net sink). Based on concentration differences, the marine system is also a sink. As temperature increases, however, plants become less efficient (around 2025) and flux eventually returns to zero at about 2075. The ocean continues to act as a sink for more than a century beyond that point. Thus, even with a doubling of atmospheric and marine carbon, the earth carbon system easily re-equilibrated. The system is a long way from a planetary boundary.

In our model, the essential dynamics reduce to how fast the ocean can pull down atmospheric carbon relative to how fast the terrestrial system loses its capacity to uptake carbon. In fact, for this parameter set, the carbon released over the industrialization process must drive the total carbon in the system over 1.71 (7,700 Pg), tripling atmospheric and marine carbon stocks. Given recent trends in carbon fluxes, it seems the earth is a long way from a planetary boundary in atmospheric carbon. Note, however, that there are many other non-linear processes and potential tipping points [*Lenton et al.*, 2008]. Two possibilities include ocean acidification that decreases a_m and landuse change releasing more carbon, increasing α. Finally, carbon could be released at a faster rate than in the scenario shown in Figure 3A as large economies develop before total emissions are curbed.

Figure 3C-D shows the potential impacts of these processes. For comparison, the scenario depicted in Figure 3A allows for roughly a quadrupling of atmospheric carbon (c_{max}=0.72, carbon stocks stabilized by 2100 before falling into the ZE region. Increasing the rate of industrialization by 50% ($r_i = 0.06$, carbon stocks stabilized in 2050), *ceteris paribus*, reduces c_{max} by 3.5%. Combining increased r_i with ocean acidification (a_m reduced from 0.04 to 0.01) and increased land clearing (α increased from 0.1 to 0.15), however, has a much stronger effect. Figure 3C shows a scenario in which society stabilizes carbon at 30% above present stocks ($c_{max} = 0.3$). As in the first scenario, as c_a increases, both the terrestrial and marine systems become sinks. However, because the marine system takes up carbon more slowly, c_a increases beyond the intersection of the photosynthesis and respiration curves in Figure 1 (around 2050). During this period, the terrestrial system becomes a net source, and the marine system remains a sink. Eventually, the marine system pulls down c_a, allowing the terrestrial system to accumulate carbon again (about 2080), and stabilize the system with c_a about double its preindustrial level. The essential dynamic hinges on whether the marine system can pull c_a down in time for the terrestrial system to re-accumulate carbon.

Figure 3D illustrates a scenario with $c_{max} = 0.42267$ (solid curves), c_a stabilizes at 1600 Pg. The dashed curves illustrate the same scenario except with $c_max = 0.42268$. The boundary between the PE and ZE basins occurs between these two values. As noted earlier, the two trajectories follow each other very closely for decades until they diverge sharply around 2100. For $c_{max} = 0.42267$ (solid) the dynamics are qualitatively the same as the scenario in Figure 3C - after losing carbon while the marine system absorbs it, the terrestrial system recovers quickly when temperature conditions permit it. For $c_{max} = 0.42268$ (dashed), on the other hand, the terrestrial system never recovers, rather, after losing carbon at a stable rate between roughly 2050 and 2100, it begins to rapidly loose carbon just after 2100. Two features might be used to detect the boundary in real time using terrestrial flux data: 1) a long period of stable flux to the atmosphere (curvature near zero, and 2) a change in curvature from convex down to convex up. Far away from the boundary, on the other hand, the curvature is strongly negative during periods of positive flux. Although clear in a deterministic model, noise and complexity in the real system would make the boundary very difficult to detect.

5. Conclusions

Using a stylized Earth System model, we explored the notion of planetary boundaries in nonlinear systems, both in state space (Figure 2A-C) and in parameter space (Figure 2F). The analysis illustrates how the resilience of the system is reduced as human activity removes carbon stocks from land systems. We next showed how increasing total available carbon stock by the release of fossil carbon causes the boundaries of this SOS to move. Finally, we clearly demonstrated the importance of the marine carbon sink in Earth System dynamics. Although we focused here on the relatively small carbon pool in the upper layers of the ocean, for longer time frames (centuries or longer) the transfer of carbon from the surface to deeper layers in the ocean becomes important. Observations that question the long-term capability of the ocean carbon sink to keep up proportionately with the rising rate of human emissions of carbon dioxide are thus of concern for avoiding unstable domains of the Earth System [*Le Quéré et al.*, 2009].

Our preliminary results suggest that the Earth System is far from a tipping point in the photosynthesis/respiration dynamics of land systems, one of the important processes in the carbon cycle that influence atmospheric carbon concentration and with it, global average temperature. However, one of the key points of our analysis is that non-linear feedbacks cause thresholds to move. Our model does not include the potential release of large amounts of methane from melting permafrost [*Schuur et al.*, 2011] or changes in albedo associated with changes in the extent of the cryosphere, two positive feedback processes that also have a major influence on the global average temperature and could move the photosynthesis/respiration dynamics boundary closer to the present location of the Earth System in state space.

The original development of the planetary boundaries concept [*Rockström et al.*, 2009] treated individual boundaries independently. Here we extend this work by exploring how interactions among boundaries can generate complex dynamics including multidimensional tipping points (Figure 3C-D). This work suggests future research directions focusing on detailed exploration of the interaction of processes that may create critical fragility regions that contain infinitely many tipping points that are almost impossible to detect. A critical question is whether a single, global tipping point might emerge from the aggregate of many local and regional tipping points. The global tipping point suggested for loss of biodiversity might indeed be an example of such an emergent global property arising from the aggregate of many smaller level nonlinear changes in biodiversity [*Barnosky et al.*, 2012].

Finally, further research with more complex Earth System models is required to test the robustness of these preliminary findings in terms of possible application to policy development [*Friedlingstein et al.*, 2006]. There is a need for

ongoing interaction between the policy and research communities to periodically reassess the individual boundaries as their interactions become better understood and as human activities change the position of the control variables on the individual boundaries.

References

Atkin, O., and M. Tjoelker, Thermal acclimation and the dynamic response of plant respiration to temperature, *Trends in Plant Science*, *8*(7), 343–351, 2003.

Barnosky, A., et al., Approaching a state shift in earth's biosphere, *Nature*, *486*, 52–58., 2012.

Bunce, J., Acclimation of photosynthesis to temperature in eight cool and warm climate herbaceous C3 species: temperature dependence of parameters of a biochemical photosynthesis model, *Photosynthesis Research*, *63*(1), 59–67, 2000.

Cabrera, H., F. Rada, and L. Cavieres, Effects of temperature on photosynthesis of two morphologically contrasting plant species along an altitudinal gradient in the tropical high andes, *Oecologia*, *114*(2), 145–152, 1998.

Cramer, W., et al., Global response of terrestrial ecosystem structure and function to co2 and climate change: results from six dynamic global vegetation models, *Global Change Biology*, *7*(4), 357–373, 2001.

Forward, D., Effect of temperature on respiration, *Encyclopedia of plant physiology*, *12*(part 2), 234–258, 1960.

Friedlingstein, P., et al., Climate-carbon cycle feedback analysis: Results from the c4mip model intercomparison, *Journal of Climate*, *19*, 3337–3353, 2006.

James, W., *Plant respiration.*, Clarendon Press, Oxford, 1953.

Kerr, R., Climate tipping points come in from the cold, *Science*, *319*(5860), 153, 2008.

Lal, R., Soil erosion and the global carbon budget, *Environment international*, *29*(4), 437–450, 2003.

Le Quéré, C., et al., Trends in the sources and sinks of carbon dioxide, *Nature Geoscience*, *2*, 831–836., 2009.

Lenton, T., Land and ocean carbon cycle feedback effects on global warming in a simple earth system model, *Tellus B*, *52*(5), 1159–1188, 2000.

Lenton, T., H. Held, E. Kriegler, J. Hall, W. Lucht, S. Rahmstorf, and H. Schellnhuber, Tipping elements in the earth's climate system, *Proceedings of the National Academy of Sciences*, *105*(6), 1786, 2008.

Mahecha, M., et al., Global convergence in the temperature sensitivity of respiration at ecosystem level, *Science*, *329*(5993), 838, 2010.

Murata, Y., and J. Iyama, Studies on the photosynthesis of forage crops II. Influence of air temperature upon the photosynthesis of some forage and grain crops, in *Proc. Crop Sci. Soc. Japan*, vol. 31, pp. 315–322, 1963.

Petoukhov, V., A. Ganopolski, V. Brovkin, M. Claussen, A. Eliseev, C. Kubatzki, and S. Rahmstorf, Climber-2: a climate system model of intermediate complexity. Part I: Model description and performance for present climate, *Climate dynamics*, *16*(1), 1–17, 2000.

Prentice, I., et al., The carbon cycle and atmospheric carbon dioxide, in *Climate Change 2001: The scientific basis. Contribution of Working Group I to the Third Assessment Report of the Intergovernmental Panel on Climate Change*, edited by J. Houghton, Y. Ding, D. Griggs, M. Noguer, P. van der Linden, X. Dai, K. Maskell, and C. Johnson, Cambridge University Press, Cambridge and New York, 2001.

Rahmstorf, S., Bifurcation of the atlantic thermohaline circulation in response to changes in the hydrological cycle, *Nature*, *378*(9), 145–149, 1995.

Randall, D., et al., Climate models and their evaluation, in *Climate Change 2007: The Physical Science Basis. Contribution of Working Group I to the Fourth Assessment Report of the Intergovernmental Panel on Climate Change*, edited by S. Solomon, D. Qin, M. Manning, Z. Chen, M. Marquis, K. Averyt, M.Tignor, and H. Miller, Cambridge University Press, Cambridge, United Kingdom and New York, NY, USA., 2007.

Rockström, J., et al., A safe operating space for humanity, *Nature*, *461*(7263), 472–475, 2009.

Roe, G., and M. Baker, Why is climate sensitivity so unpredictable?, *Science*, *318*(5850), 629, 2007.

Schuur, E., B. Abbott, and the Permafrost Carbon Network, High risk of permafrost thaw, *Nature*, *480*, 32–33, 2011.

Tjoelker, M., J. Oleksyn, and P. Reich, Modelling respiration of vegetation: evidence for a general temperature-dependent q10, *Global Change Biology*, *7*(2), 223–230, 2001.

Yuan, W., et al., Redefinition and global estimation of basal ecosystem respiration rate, *Global Biogeochemical Cycles*, *25*(4), GB4002, 2011.

J. M. Anderies School of Sustainability and School of Human Evolution and Social Change Arizona State University P.O. Box 872402, Tempe, AZ 85287-2402 (m.anderies@asu.edu)

Appendix A: Model details

This supplement provides details of the model development. Specifically, we provide the scientific basis for the function $NEP(p(T, c_a(t)), r(T), c_t(t))$ in Equation (1) in the main document. This function is the core driver of the model dynamics. Next, we provide intermediate analysis of a lower dimensional version of the model which excludes marine stocks. This intermediate analysis provides some intuition for the dynamics before we analyze the full model. Again, the model is similar in spirit to the Earth System model of *Lenton* [2000] and captures interactions between Net Ecosystem Production (NEP) and terrestrial, marine, and atmospheric carbon stocks (Figure S1). We begin developing the relationships between temperature, photosynthesis, and respiration, then link these relationships to atmospheric carbon stocks. Finally, we describe the model for carbon fluxes between stocks.

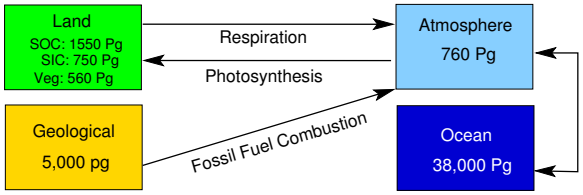

Figure S1. Minimal model depiction of the Earth System in terms of the relations between carbon stocks (stock data from *Lal* [2003]).

A1. Temperature Relationships

The key relationships considered are between air temperature, photosynthesis and respiration (at the ecosystem level) and between air temperature (without considering complicating geophysical factors) and carbon concentration in the atmosphere. Photosynthesis and respiration are affected by many factors but at the most basic level, studies suggest that both respiration and photosynthesis rates will increase with temperature when temperatures are low and then begin to decrease beyond some physiologically set threshold. These relationships are formalized as follows:

Photosynthesis: The basic hump-shaped relationship between photosynthesis (net carbon assimilation rate in μ mol/m^2 s) and temperature has been demonstrated for a number of plant species [*Bunce*, 2000; *Cabrera et al.*, 1998; *Murata and Iyama*, 1963]. Here we use a simple function,

$$f(T; a, b, c) = a(T)^b \exp(-c(T)) \tag{A1}$$

to capture this relationship. The parameters a, b, and c, are chosen to fit the general features of temperature-photosynthesis relationships from the literature. Thus, we let $p(T) = f(T; a_p, b_p, c_p)$ where $p(T)$ is photosynthesis as a function of temperature, T. Note that this relationship can be specified in terms of leaf temperature [.e.g *Cabrera et al.*, 1998] or air temperature in a controlled volume during photosynthesis [e.g. *Murata and Iyama*, 1963]. For our purposes, this must be adjusted to an annual mean temperature for consistency with temperature-respiration relationships as discussed below. An example of $p(T)$ is shown by the solid curve in Figure S2A.

Respiration: Mahecha et al. [2010] suggest that at the ecosystem level, temperature sensitivity of respiration rate is constant, i.e. $Q_{10} \approx 1.4$, globally. Thus respiration increases exponentially with increasing temperature. However, over shorter time scales (minutes to hours), Q_{10} has been shown to decrease linearly with temperature [*Tjoelker et al.*, 2001; *Forward*, 1960; *James*, 1953]. In this case, the temperature-respiration relationship would have the shape of the dashed curve in Figure S2A for $T < 18$. [cf. *Atkin and Tjoelker*, 2003]. Although the basic chemical reaction that drives respiration [e.g. *Lenton*, 2000] may allow for respiration rates to increase indefinitely, at some point high temperatures may affect the physical system that supports the reaction thereby reducing the efficiency with which the reaction can be carried out. This suggests that the temperature-respiration would bend over at high temperatures as in the dashed curve in Figure S2A for $T > 18$. Recent work by *Yuan et al.* [2011] provides evidence that this is indeed the case. Again, the function $f(T; a, b, c)$ defined by (A1) is sufficiently general to capture this relationship, and we let $r(T) = f(T; a_r, b_r, c_r)$. The dashed curve in S2A shows an example in which a_r, b_r, c_r, and the temperature scaling have been chosen to match the basic relations reported in [*Yuan et al.*, 2011]. The temperature axes should be interpreted as mean annual nocturnal air temperature. It is important to note that the details of these functional forms is not critical to the qualitative dynamics for the system. The important feature is that for some temperature range $p(T) > r(T)$. Otherwise, terrestrial ecosystems could never accumulate carbon (biomass), i.e. NEP would always be negative.

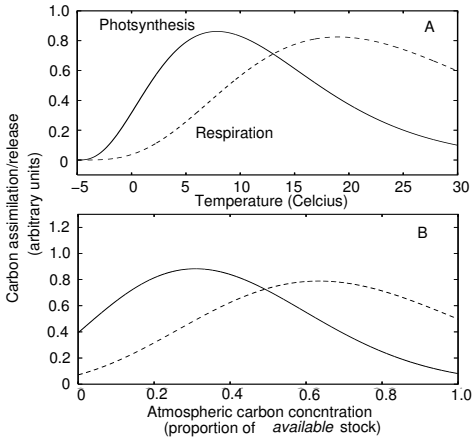

Figure S2. A: Temperature, photosynthesis, and respiration relations. Parameter values: $a_1 = 220$, $b_1 = 3$, $c_1 = 7$, $a_2 = 110$, $b_2 = 4$, $c_2 = 5$. Temperature scale is arbitrary and was chosen to correspond to data from the literature. The functions plotted are $f((x+5)/30, ...)$. B: Same relations as a function of atmospheric carbon. The fertilization effect parameters are $c_f = 1.5$, and $b_f = 0.3$. Figure S3 illustrates the effect of different choices of the fertilization parameters on the model.

A2. Atmospheric Carbon and NEP

CO_2 affects NEP in two ways: indirectly through temperature (both photosynthesis and respiration) and directly through a fertilization affect. Given the uncertainty associated with changes in radiative forcing associated with CO_2 concentrations and changes in global and annual mean temperature [*Roe and Baker*, 2007], we make only the most basic assumption: annual mean temperature (in the absence of feedbacks between different carbon stocks) increases linearly with CO_2. If we define $c_a(t)$ as the atmospheric carbon concentration at time t, then we have

$$T(c_a(t); a_T, b_T) = a_T c_a(t) + b_T \tag{A2}$$

where, again, a_T and b_T are arbitrary parameters. Substitution of (A2) into the expressions for $p(T)$ and $r(T)$ leads to a family of mappings between c_a, photosynthesis, and respiration, i.e.

$$p(c_a(t)) = f(T(c_a(t); a_T, b_T); a_p, b_p, c_p) \tag{A3}$$
$$r(c_a(t)) = f(T(c_a(t); a_T, b_T); a_r, b_r, c_r) \tag{A4}$$

that have the forms shown in Figure S2B.

Regarding the fertilization effect of atmospheric carbon, the simplest assumption we can make as that increasing carbon increases photosynthetic activity, recognizing the fact that other limiting factors will eventually begin to reduce the effects of additional CO_2 in the atmosphere. This implies that $\partial p/\partial c_a > 0$ and $\partial^2 p/\partial c_a^2 < 0$. A very simple function that exhibits such behavior is

$$g(x; a_f, b_f) = c_f x^{b_f} \tag{A5}$$

where $0 < b_f < 1$ and $c_f > 0$ are parameters. This functional form has the basic shape associated with Michaelis-Menten kinetics assumed in *Lenton* [2000]. Assuming a multiplicative relation between temperature and carbon fertilization effects [again, as in *Lenton*, 2000] and writing

$$f_p(c_a) = f(T(c_a(t); a_T, b_T); a_p, b_p, c_p) \tag{A6}$$

(suppressing parameters and time dependence for clarity) we can rewrite (A3) and (A4) as

$$p(c_a) = g(c_a) f_p(c_a) \tag{A7}$$
$$r(c_a) = f_r(c_a). \tag{A8}$$

A3. Carbon dynamics

Given the definitions of how carbon flows in ($p(c_a)$) and out ($r(c_a)$) of terrestrial systems as a function of atmospheric carbon concentration (c_a) given by (A7) and (A8), we are now in a position to specify the relationship between the different carbon stocks shown in Figure S1. We will do this in two stages to provide intuition for the analysis of the full model. We first consider the interaction between terrestrial and atmospheric stocks only and explore the affect of some key parameters on the dynamics. We then add marine and geological stocks and present an analysis of the full model.

Equations (A7) and (A8) define carbon flow rates per some unit of plant biomass. Neglecting the complexities of the terrestrial carbon cycle for the moment and assuming that plant biomass is linearly related to terrestrial carbon we have

$$NEP(p(T, c_a(t)), r(T), c_t(t)) = r_{tc} c_t (p(c_a) - r(c_a)) \tag{A9}$$

where r_{tc} is an ecosystem-dependent conversion factor. Assuming no human impacts for the moment, the simplest model for the change in terrestrial carbon stores is

$$\frac{dc_t}{d_t} = r_{tc} c_t (p(c_a) - r(c_a)). \tag{A10}$$

We explore the implications of this simple representation considering only terrestrial and atmospheric stocks. Conservation of mass implies that $c_a + c_t = C$ where c_t and C are the terrestrial and total carbons stocks, respectively. Substituting $C - c_t$ for c_a in (A10) yields the following first-order, autonomous, nonlinear ordinary differential equation

$$\frac{dc_t}{d_t} = r_{tc} c_t (p(C - c_t) - r(C - c_t)). \tag{A11}$$

Figure S3 shows the right hand sides of (A11) with total carbon normalized to 1 for different values of b_f (A) and c_f (B) which characterize the fertilization effect. b_f is a measure of the sensitivity of plants to changing atmospheric carbon concentration. Small values of b_f imply that plants respond quickly to increasing carbon concentrations but saturate rapidly - i.e. become insensitive to carbon (blue curve, top, Figure S3). For large values of b_f, plants respond more slowly, but continue to respond across a larger range of carbon concentrations (red curve, top, Figure S3). These curves have three roots (equilibrium points where $dc_t/dt = 0$). Roots indicated with boxes and circles are unstable and stable, respectively. The direction of motion of terrestrial carbon stocks is shown in the bottom graph (to avoid clutter). For initial conditions to the right of the unstable equilibria, the system will converge to a state with high terrestrial carbon concentrations, in a cold climate, with a low carbon atmosphere, and very low rates of photosynthesis and respiration (e.g. perpetual tundra with lots of peat bogs and hydrocarbon reserves). For those to the left, the system converges to a state with no terrestrial organic carbon and an extremely hot climate (e.g. a global desert).

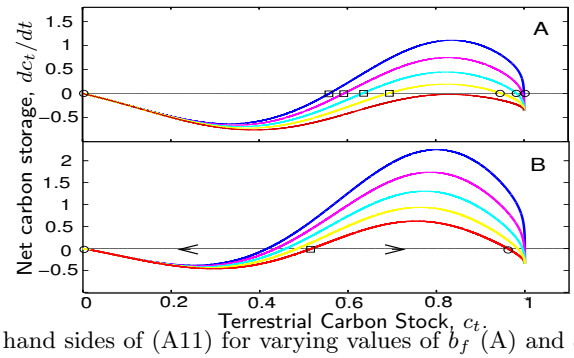

Figure S3. Examples of right hand sides of (A11) for varying values of b_f (A) and c_f (B).

Given other constraints on terrestrial carbon dynamics (e.g. water), we would not expect to see the all-or-nothing result shown in Figure S3. The figure does, however, illustrate the tension between temperature and fertilization effects. The more sensitive to carbon fertilization effects, the more atmospheric carbon is required for growth. This however, has a negative effect through increased temperature. Thus the system represented by the yellow curve has a narrower survival range than that represented by the blue curve. The curves in the bottom graph show the effect of increasing the overall effect of fertilization relative to temperature effects. The curves represent the same values of b_f (color coordinated) but c_f is 50% larger in the bottom plots. The benefits of atmospheric carbon through fertilization allow for a broader terrestrial biomass survival range by shifting the unstable equilibrium to the left.

To avoid the unrealistic dichotomy of either frozen tundra or burning desert, the model can be easily extended to incorporate other constraints on carbon dynamics such as water and land availability. This is accomplished by adding density dependence in terrestrial carbon (land systems can only support so much biomass). This simplest way to do this is add a carrying capacity term and modify (A11) as follows:

$$\frac{dc_t}{d_t} = r_{tc}(p(C - c_t) - r(C - c_t))(1 - \frac{c_t}{k}) \tag{A12}$$

where the parameter k sets an upper limit on the terrestrial biomass that can be supported. Examples of $\frac{dc_t}{d_t}$ generated by (A12) are shown in Figure S4A.

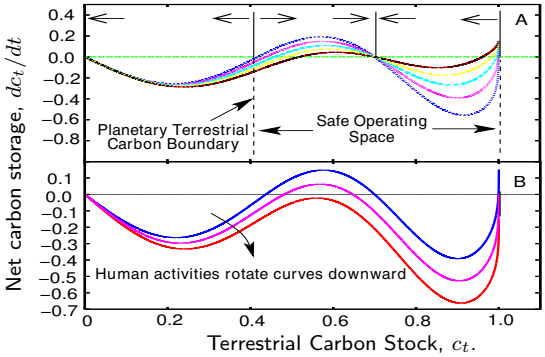

Figure S4. Examples of right hand sides of (A12) for varying values of b_f (A). Examples of right hand sides of (A13) for varying values of α (B).

Density dependence introduces a new stable equilibrium at $c_a = k$. The dynamics are illustrated with arrows on Figure S4 (A). Now there are 4 equilibria, two stable and two unstable. With this formulation, we can describe the idea of a planetary boundary in terms of land use. This simple model does not capture the complexity of land use, of course, but may (or slightly more complex models like it) correctly describe the issue of moving boundaries, and an SOS defined by feedbacks. The boundary and corresponding SOS shown correspond to the blue curve (strongest fertilization effect). The system can tolerate reductions in terrestrial carbon (and corresponding increases in atmospheric carbon) to roughly 0.41 (corresponding to 0.59 in atmosphere). Given that the equilibrium is 0.7, we can compute the size of the basin of attraction, or specified resilience as 0.29. Now are now in a position ask how human activities affect the boundary and the resilience of the system.

We introduce human activity through a terrestrial carbon offtake term, $H(t)$, i.e. clearing, burning, or farming techniques that reduce the carbon sequestration capacity of terrestrial systems. We simply assume that human appropriate a certain proportion of terrestrial biomass in each time period and let $H(t) = \alpha c_t(t)$ where αc_t is the offtake rate. To arrive at our final model, we modify (A12) to read

$$\frac{dc_t}{d_t} = r_{tc}(p(C - c_t) - r(C - c_t))(1 - \frac{c_t}{k}) - \alpha c_t \tag{A13}$$

Figure S4 (B) shows the affect of human carbon offtake. As α increases, the SOS shrinks and eventually vanishes. We can compute when this occurs (peak of curve falls below horizontal - e.g. red curve, Figure S4) using bifurcation techniques. If α exceeds 26% of terrestrial carbon stocks, the system enters the "hot desert" (HD) basin.

Equation (A13) is the model used for terrestrial carbon dynamics in the full model. We couple this with a very simple model of marine carbon dynamics (see main document) to generate a 2-dimensional model that is used for analysis in the main document. The simple analysis presented here should provide some intuition for what is happening in the more-difficult-to-visualize full model.